Geothermal Resources Council *Transactions*, Vol. 22, September 20-23, 1998

CO_2 Flux Measurements Across Portions of the Dixie Valley Geothermal System, Nevada

Deborah Bergfeld[1], Fraser Goff[1], Cathy J. Janik[2], Stuart D. Johnson[3]
[1]Earth and Environmental Sciences Division Los Alamos National Laboratory, NM 87545
[2]U.S. Geological Survey 345 Middlefield Rd, Menlo Park CA 94025
[3]Oxbow Power Services Reno, NV 89511

ABSTRACT

A map of the CO_2 flux across a newly formed area of plant kill in the NW part of the Dixie Valley geothermal system was constructed to monitor potential growth of a fumarole field. Flux measurements were recorded using a LI-COR infrared analyzer. Sample locations were restricted to areas within and near the dead zone. The data delineate two areas of high CO_2 flux in different topographic settings. Older fumaroles along the Stillwater range front produce large volumes of CO_2 at high temperatures. High CO_2 flux values were also recorded at sites along a series of recently formed ground fractures at the base of the dead zone. The two areas are connected by a zone of partial plant kill and moderate flux on an alluvial fan. Results from this study indicate a close association between the range front fumaroles and the dead zone fractures.

Introduction

The Dixie Valley geothermal field in west-central Nevada feeds a double-flash power plant that produces 62 MWe of power. Over the past ten years the field has undergone decreases in reservoir levels and fluid pressures in spite of reinjection of spent geothermal fluids at locations along the margin of the production zone. Other changes in the physical character of the system include enlargement in the extent and vigor of a fumarole field along the range front Stillwater fault zone north west of the field, the formation of an area of plant kill (the dead zone), and growth of a series of ground fractures.

The geothermal power plant at Dixie Valley is owned and operated by Oxbow Geothermal Corporation. In 1996 a team of researchers from Los Alamos Laboratory and Lawrence Livermore Laboratory was formed to investigate scaling problems in injection lines. In 1997 the team was joined by the U.S. Geological Survey and the early study was expanded to a larger geochemical investigation of the geothermal fluids and local and regional groundwaters. The goals of this study are to characterize recharge to the geothermal system, provide geochemical monitoring of reservoir fluids and to examine the temporal and spatial distribution of the CO_2 flux in the dead zone. This paper reports the results of the initial CO_2 flux measurements taken in October, 1997.

Geologic Setting

Dixie Valley is an asymmetric, northeast trending graben bounded by the Stillwater Range on the west and the Clan Alpine Range on the east (Anderson et al., 1983; Waibel, 1987; Honjas et al., 1997; Lutz et al., 1997). The geothermal field is located along the western, deeper margin of Dixie Valley near the Stillwater fault. Thicknesses of Tertiary basin fill sediments are up to 2000 m in geothermal wells (Forster et al., 1997). Movement along the presently active Stillwater fault has produced roughly 2.9 km of offset between the Stillwater range and Dixie Valley over the past 10 Ma (Okaya and Thompson, 1985). As such, the rocks units exposed in the Stillwater range are the same as those penetrated by geothermal wells in the basin. They consist of repeated, thrust-related sequences of Triassic and Jurassic marine metasedimentary rocks and a Jurassic gabbro that were later intruded by a Cretaceous granodiorite. The Mesozoic rocks are unconformably overlain by the Miocene Table Mountain Basalt. In the basin this basalt hosts the upper geothermal reservoir at depths between 2300 to 2700 m (Lutz et al., 1997). The main geothermal reservoir between 2830 to 3330 m is hosted in fractured Jurassic rocks within the hanging wall of the Stillwater fault (Lutz et al., 1997). Average temperatures of reservoir fluids are about 250°C.

The recently identified dead zone located in the northwestern part of the geothermal field extends from the Senator fumarole southeast into the valley (Fig. 1). The area of partial to total plant kill first identified in fall 1995 spreads over a nearly 1 km^2 region of alluvial fan and basin sediments. Plants that grow in the area consist primarily of low lying woody shrubs (greasewood and shadscale) and grasses. Plant mortality across the upper fan is patchy with increasing die-off at locations near a road at the fan terminus. The southernmost of two sets of ground fractures is also located near the fan-valley margin. Depth of the cracks varies from centimeters to around 0.5 meter. Soil in the cracks is moist and soil temperatures at the bottom of these cracks are ≤ 96°C (Fig. 2). During cool, moist periods of the day steam can be seen rising from this area. At the ground surface adjacent to the cracks a thin crust of unidentified mineral precipitates is commonly observed. Plant mortality in this "steaming ground" region is almost 100%.

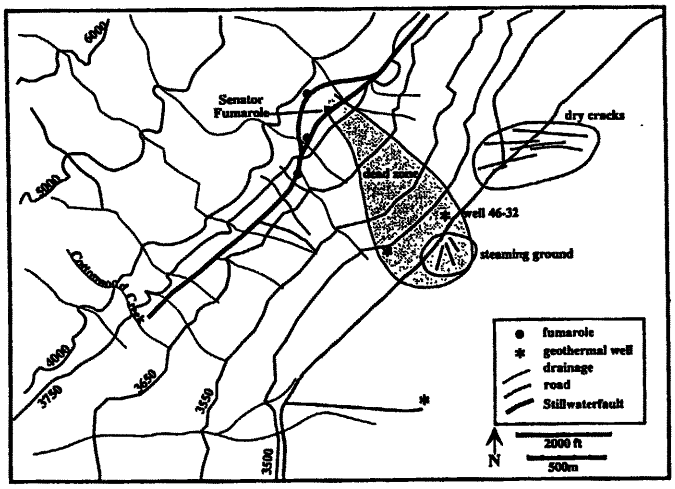

Figure 1. Generalized map of the dead zone area showing the location of geothermal wells, ground fractures and fumaroles along the Stillwater fault zone.

The second set of ground cracks (Fig. 3) is located in basin-fill sediments northeast of the steaming ground. These cracks are generally oriented in an east-west direction. The soil within the cracks is dry with average temperatures of about 17°C. In comparison with the cracks in the steaming ground these cracks are more strongly oriented, more laterally extensive, and are deeper. The plants around these "dry cracks" are healthy.

Methods

Early CO_2 soil gas investigations at geothermal areas have been conducted much like helium and mercury surveys in which gas or soil samples were collected over a target area and analyzed in a laboratory (e.g., McCarthy, 1983). In these investigations, CO_2 concentration was measured rather than CO_2 flux. More recently, CO_2 soil gas investigations resembling the type described herein have been conducted in volcanic areas to investigate sudden increases in CO_2 flux associated with recent tree/plant kills (Farrar et al., 1995; McGee and Gerlach, 1998; Gerlach et al., 1998), to estimate

Figure 2. Photo of the steaming ground at the southeastern limit of the dead zone. All shrubs are dead.

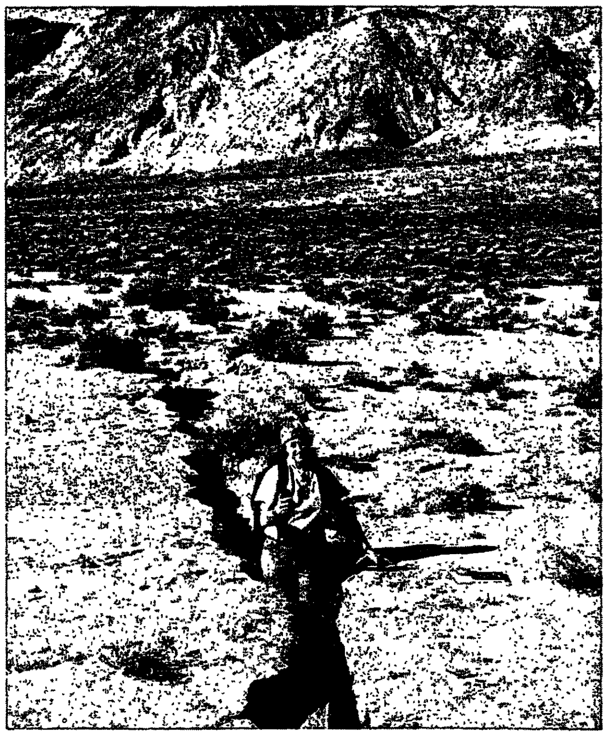

Figure 3. Photo of the dry cracks. Shrubs are brown during the winter but are alive.

total volcanic CO_2 flux from volcanic vents and diffuse flank emissions (Allard et al., 1991; Chiodini et al., 1996), and to identify tectonic structures associated with volcanic degassing (Barberi and Carapezza, 1994; Giammanco and Gurrieri, 1997).

Soil CO_2 concentrations for the Dixie Valley study are measured using a LI-COR brand infrared gas analyzer. The analyzer is used in a closed loop with an accumulation chamber and is equipped with a soda lime cartridge to scrub CO_2 from the chamber. The gas analyzer is linked to a microcomputer that controls data logging and storage, and performs the flux calculations. For this study flux is calculated as grams of CO_2 per m^2 per day. The gas analyzer is calibrated at least once a day using a reference gas. Atmospheric pressure is monitored as variation may affect the calibration. Any change in pressure is noted and accounted for in the computer program.

Prior to taking a soil CO_2 measurement a reading of the ambient air CO_2 concentration at the soil surface is obtained. The accumulation chamber is then placed over the site and the gas is routed through the soda lime to scrub the chamber gas to CO_2 concentrations below ambient. Once an appropriate CO_2 concentration is achieved, the soda lime is bypassed and CO_2 concentration in the chamber begins to rise. The data used in the flux calculations are logged from CO_2 concentrations below, to just above ambient. This method reduces the chance for diffusion into or out of the chamber.

Sites for flux measurements were selected along regularly spaced traverses that enclose the dead zone. Additional traverses were located along and across splays in the Stillwater fault and around the dry cracks area. Several short traverses were located in the basin away from the dead zone. Soil temperature data were collected at the same time that gas data were obtained. Flux measurements directly over fumaroles were not obtained as CO_2 concentrations immediately rise to levels beyond the measurement capabilities of the analyzer. The data are contoured with a software package that uses kriging statistics to provide a minimum error estimate of an evenly spaced data set. As a result of the contouring, localized extremely high flux values are depressed on the resulting map.

CO_2 Flux

Measurements of diffuse soil CO_2 flux show no anomalous CO_2 associated with the dry cracks area (Fig 4). Average flux at these sites is 1.8 g/m^2/d, similar to other basin measurements away from the steaming ground. This value is low compared to a prairie soil (about 8-11 g/m^2/d, Norman et al., 1992) and essentially defines the background flux for the local basin-fill sediments. Flux measurements across the dead zone show two areas with relatively high flux. Sites along the Stillwater fault and near the cracks in the steaming ground area have maximum fluxes around 200 and 170 g/m^2/d. The flux rapidly declines away from individual high-flux point sources but all sites in these areas yield values well above the local background.

The contoured data show two trends identified by high CO_2 flux values. A SW-NE trend parallel to the range front is located along the fumaroles in the fault zone. It is likely that this area produces the largest volume of CO_2 compared to any part of the dead zone but more data are required before these calculations can be attempted. The second trend in the flux data is oriented at a high angle to the fault zone and lies within the body of the dead zone. This "dead zone" trend is anchored by locations near the fumaroles and the steaming ground but is also delineated by enhanced CO_2 flux values in the mid-fan region.

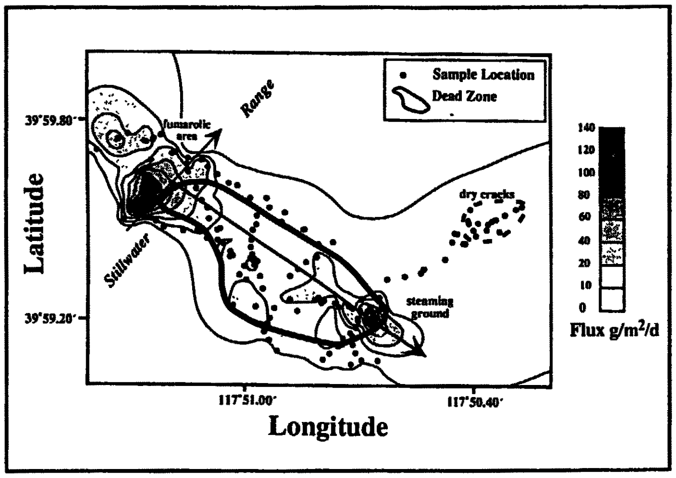

Figure 4. Contour map of the soil CO_2 flux data. Large arrows delineate the trends defined by elevated CO_2 flux. The Stillwater trend (oriented NE) is located along the Stillwater fault zone. The dead zone trend (oriented SE) connects the fumaroles with the steaming ground and is oriented at a high angle to the Stillwater trend.

Soil Temperatures

The contour map of the soil temperature data (Fig. 5) is strikingly similar to the flux contour map. These data imply that the source of the thermal signature in the dead zone is closely associated with the processes that generate the high concentrations of CO_2. As with the flux data, soil temperatures around the dry cracks show no anomaly associated with the ground fractures. At depths of 6 cm soil temperatures for the basin sediments are about 17°C. In contrast, locations along the fault trend and within the steaming ground area show a strongly elevated thermal signature. Temperatures in these areas are highly variable between 18 to 66°C with average temperatures around 20°C higher than the normal basin soils. Soil temperature data from the mid portion of the dead zone are less variable and are on average elevated above background temperatures.

Discussion

The NW-SE alignment of the dead zone high flux trend is parallel to the direction of the present-day least horizontal principal stress (Hickman and Zoback, 1997), and is dissimilar to the orientation of major and subsidiary faults that are believed to control fluid flow in the Dixie Valley reservoir. Older NNW oriented faults related to early extension are often sericitized and may be poor conduits for fluids (Lutz et al., 1997). At locations south of the geothermal field active and fossil hot spring activity has been observed at intersections of the NNW faults with parts of the Stillwater fault (Lutz et al., 1997).

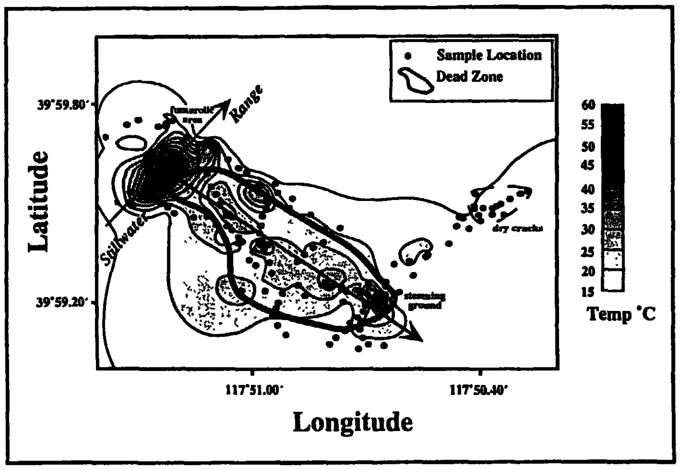

Figure 5. Contour map of the soil temperature data. Large arrows delineate the Stillwater and dead zone trends defined by elevated soil temperatures.

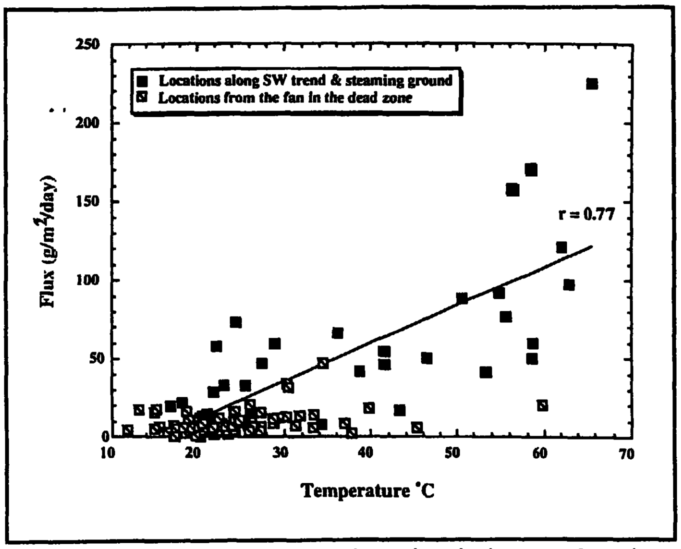

Figure 6. Plot of flux-temperature relationships for locations from this study. Regression is through the samples from the Stillwater trend and the steaming ground. Locations along the fan portions of the dead zone show little relationship between flux and soil temperature. Samples from basin-fill sediments were omitted for clarity.

The recent development of two separate areas of ground fractures argues for a common factor in their formation. However, background levels of CO_2 flux and normal soil temperatures indicate that the dry cracks are not likely related to expansion of the fumarole field and are more likely related to subsidence within the basin. In contrast, the fractures across the steaming ground have features in common with the older fumaroles along the range front. The relative magnitudes of the CO_2 flux around individual point sources are comparable (Fig. 4). In addition, the correlation between the temperature and flux data is most strongly expressed by these two high-flux areas. Figure 6 shows a linear regression of the combined data from locations along the Stillwater trend and from sites within the steaming ground r = 0.77). Sample locations along the fan in the dead zone also have an elevated flux but these sites have a much lower correlation with temperature r = 0.37).

In the steaming ground area soil temperatures at 6 cm depth range between 23°C near live plants to 62°C near steaming cracks. As previously mentioned, temperatures at the base of these cracks (≈ 0.5m) are around 96°C; the boiling point for this elevation is about 97°C. The large variations of surface soil temperatures around the steaming ground area suggest that heat flow is focused by fracture permeability. An estimate of the localized shallow geothermal gradient can be calculated from temperature data obtained in well 46-32 which is 155°C at 87m (depth at the static water level). The thermal gradient calculated for the lower dead zone using the temperatures from this well and those at the base of the cracks is 680°C/km. By assuming a thermal conductivity around 1.6 W/m°C for the basin fill, the heat flow for the lower dead zone is around 1100 mW/m^2 (≈ 26 HFU). For comparison, Sulphur Springs, an area of acid-sulfate springs and fumaroles in Valles caldera has a measured heat flow of 1300 to 7200 mW/m^2 (Morgan et al., 1996). Normal regional heat flow values for Dixie Valley are between 90 to 110 mW/m^2 with higher values around 140 mW/m^2 in zones of upward fluid flow along the Stillwater fault zone (Williams et al., 1997).

As yet the causes of the steaming ground fractures are unknown. Increased activity at Senator fumarole, formation of new fumaroles and ground cracks, and development of the dead zone suggest that changes are occurring in the upper levels of the northern sector (Section 33 Wells) of the Dixie Valley geothermal system. While there is no evidence at this time that these upper level changes are related to reservoir fluid production and drawdown, the coincidence of events is potentially noteworthy. Hydrothermal eruption craters and breccias are a common feature in the Recent geologic record of many high-temperature geothermal systems (Muffler et al., 1971; Hedenquist and Henley, 1985). Explosions have occurred in producing geothermal fields (Scott and Cody, 1982; Bruno et al., 1992), and increased fumarolic activity caused by production is occasionally a precursor to small hydrothermal explosions (Bixley and Browne, 1988). While the causes of such explosions are varied and the modeling complicated (McKibben, 1989), prudence and safety dictate that increasing fumarole activity in geothermal areas is a potential hazard worthy of surveillance. The CO_2 flux and temperature measurements provide tools to extend reservoir monitoring capabilities to areas outside of the production and injection zones.

Acknowledgments

This research is funded by the Geothermal Division, U.S. Department of Energy (Marshal Reed). We thank Oxbow Geothermal Corporation for access to the sites and for approving publication of this paper. In addition we thank Giday WoldeGabriel and Alfred Truesdell for their thoughtful reviews of this paper.

References

Allard, P., Carbonnelle, J., Dajlevic, D., Le Bronic, J., Morel, P., Robe, M.C., Maurenas, J.M., Faivre-Pierre, R., Martin, D., Sabroux, J.C., and Zettwoog, P., 1991. Eruptive and diffuse emissions of CO_2 from Mount Etna. Nature, 351, p. 387-391.

Anderson, R.E., Zoback, M.L., and Thompson, G.A., 1983. Implications of selected subsurface data on the structural form and evolution of some basins in the northern Basin and Range province, Nevada and Utah. Geol. Soc. of Amer. Bull., 94, p. 1055-1072.

Barberi, F., and Carapezza, M.L., 1994. Helium and CO_2 soil gas emission from Santorini (Greece). Bull. Volcanol. 56, p. 335-342.

Bixley, P.F., and Browne, P.R.L., 1988. Hydrothermal eruption potential in geothermal development. Proceedings, 10th New Zealand Geothermal Workshop, Geothermal Institute, Univ. Auckland, p. 195-198.

Bruno, C.A.E., Burgos, J.A., and Ayala-M., S., 1992. Agua Shuca hydrothermal eruption. Geotherm. Resourc. Counc. Bull., Dec., 1992, p. 361-369.

Chiodini, G., Frondini, F., and Raco, B., 1996. Diffuse emission of CO_2 from the Fossa crater, Vulcano Island (Italy). Bull. Volcanol., 58, p. 41-50.

Farrar, C.D., Sorey M.L., Evans W.C., Howle J.F., Kerr, B.D., Kennedy, B.M., King, C.Y., and Southon J.R., 1995. Forest-killing diffuse CO_2 emission at Mammoth Mountain as a sign of magmatic unrest. Nature 376, p. 675-678.

Forster, C.B., Caine, J.S., Schulz, S., and Nielson, D.L., 1997. Fault Zone Architecture and Fluid Flow: An Example from Dixie Valley, Nevada. Proceedings of the 22nd Workshop on Geothermal Reservoir Engineering, Stanford University Report SGP-TR-155, Stanford, California, January 27-29, p. 123-130.

Gerlach, T.M., Doukas, M.P., McGee, K.A., and Kessler, R., 1998. Three-year decline of magmatic CO_2 emissions from soils of a Mammoth Mountain tree kill: Horseshoe Lake, CA, 1995-1997. Geophy. Res. Lett, 25, p. 1947-1950.

Giammanco, S., and Gurrieri, S., 1997. Soil CO_2 degassing along tectonic structures of Mount Etna (Sicily): the Pernicana fault. Applied Geochemistry, 12, p. 429-436.

Hedenquist, J., and Henley, R., 1985. Hydrothermal eruptions in the Waiotapu geothermal system, New Zealand: Their origin, associated breccias, and relation to precious metal mineralization. Econ. Geol., 80, p. 1640-1668.

Hickman, S., and Zoback, M., 1997. In-situ stress in a fault-hosted geothermal reservoir at Dixie Valley, Nevada. Proceedings of the 22nd Workshop on Geothermal Reservoir Engineering, Stanford University Report SGP-TR-155, Stanford, California, January 27-29, p. 141-146.

Honjas, W., Pullammanappillil, S.K., Lettis, W.R., Plank, G.L., Louie, J.N. and Schweichert, R., 1997. Predicting subsurface structure within the Dixie Valley geothermal field, Dixie Valley, Nevada, using a non-linear optimization scheme. Geothermal Resources Council Bulletin, February, p. 45-52.

Lutz, S.J., Moore, J.N., and Benoit D., 1997. Geologic framework of Jurassic reservoir rocks in Dixie Valley Geothermal Field, Nevada: Implication from hydrothermal alteration and stratigraphy: Proceedings of the 22nd Workshop on Geothermal Reservoir Engineering, Stanford University Report SGP-TR-155, Stanford, California, January 27-29, p. 131-139.

McCarthy, K.P., 1983. A helium exploration survey in the Animas Valley, Colorado: Geothermal Resources Council Transactions, 7, p. 311-314.

McGee, K.A., and Gerlach, T.M., 1998. Annual cycle of magmatic CO_2 at Mammoth Mountain, California: Implications for soil acidification. Geology, 26, p. 463-466.

McKibben, R., 1989. An attempt at modeling hydrothermal eruptions. Proceedings, 11th New Zealand Geothermal Workshop, Geothermal Institute, Univ. Auckland, p. 267-273.

Morgan, P., Sass, J.H., and Jacobson R.D., 1996. Heat flow in VC-2A and VC-2B, and constraints on the thermal regime of the Valles Caldera, New Mexico. New Mexico Geol. Soc. Guidebook, 47th Field Conf., Jemez Mountain Region, Socorro, NM, p. 231-236.

Muffler, L.J.P., White, D.E., and Truesdell, A.H., 1971, Hydrothermal explosion craters in Yellowstone National Park: Geol. Soc. Amer. Bull., v. 82, p. 723-740.

Norman, J.M., Garcia, R., and Verma, S.B., 1992. Soil Surface CO_2 Fluxes and the Carbon Budget of a Grassland. J. of Geophy. Res., 97 D17, p. 18,845-18,853.

Okaya, D.A., and Thompson, G.A., 1985. Geometry of Cenozoic extensional faulting: Dixie Valley: Tectonics, 4, p 107-125.

Scott, B.J., and Cody, A.D., 1982. The 20 June 1981 hydrothermal explosion of Tauhara geothermal field, Taupo: New Zealand. Geological Survey Rept. 103, 32 p.

Waibel, A.F., 1987. An overview of the geology and secondary mineralogy of the high temperature geothermal system in Dixie Valley, Nevada: Geothermal Resources Council Transactions, 11, p. 479-486.

Williams, C.F., Sass J.H., and Grubb, F.V., 1997. Thermal signature of subsurface fluid flow in the Dixie Valley geothermal field, Nevada. Proceedings of the 22nd Workshop on Geothermal Reservoir Engineering, Stanford University Report SGP-TR-155, Stanford, California, January 27-29, p. 161-168.